

# Separation of Arsenic from the Antimony-Bearing Dust through Selective Oxidation Using CuO



DA-PENG ZHONG, LEI LI, and CHENG TAN

A pyrometallurgical process of selective oxidation roasting of the antimony-bearing dust using CuO is put forward, in which the antimony component is oxidized to  $Sb_2O_4$  staying in the roasted residue, and arsenic is volatilized in the form of  $As_2O_3$ . The addition of CuO has an active effect on the arsenic volatilization, because structures of some complicated As-Sb phases in the dust are destroyed after the “Sb” component in them is oxidized to  $Sb_2O_4$ , and this part of arsenic might be transformed to  $As_2O_3$ , which continues to volatilize. However, the arsenic volatilization rate decreases with the CuO amount in a certain range, which is attributed to the greater formation of  $Cu_3(AsO_4)_2$  and  $Cu_3As$ . Under the conditions of roasting temperature of 673 K (400 °C), roasting time of 100 minutes, CuO amount of 34.54 mass pct, and  $N_2$  flow rate of 30 mL/min, 91.50 pct arsenic and only 8.63 pct antimony go into the smoke.

DOI: 10.1007/s11663-016-0896-2

© The Minerals, Metals & Materials Society and ASM International 2017

## I. INTRODUCTION

THE reserve amount of antimony in the world is higher than 2 million tons, most of which is found in China, Bolivia, Russia, South Africa, and Tajikistan.<sup>[1,2]</sup> Among them, China has the most abundant antimony resource and the current mine production is about 100,000 t/year.<sup>[3,4]</sup> However, the uncontrolled exploitation will result in it being depleted in 10 years. It is necessary to find other resources to extract antimony, in addition from the ore. There is an antimony-bearing dust generated in many pyrometallurgical processes, which also contains other valuable metals, such as lead, antimony, and indium.<sup>[5–8]</sup> Nevertheless, arsenic, a toxic element companioned with antimony,<sup>[9–12]</sup> reduces the antimony product quality if it is not removed.<sup>[13–15]</sup> In addition, this dust cannot be directly recycled to the smelters or converters because of the increase of required energy for the smelting or converting process. It is necessary to treat the dust separately to recover valuable metals.

The conventional treatment of antimony-bearing dusts can be classified into two methods: pyrometallurgical<sup>[11,16–19]</sup> and hydrometallurgical processes. The pyrometallurgical process generally involves oxidizing roasting, reduction roasting, and chlorination roasting. The  $As_2O_3$  is easy to volatilize due to its strong volatility, as a result of which the volatilization rate of it exceeded 93 mass pct in 120 minutes at 733 K (460 °C)

in one study.<sup>[20]</sup> The  $Sb_2O_3$  volatilizes in the form of  $Sb_4O_6$  (g), and its volatilization rate outstrips 95 mass pct in 140 minutes at 873 K (600 °C) under nitrogen atmosphere.<sup>[21]</sup> However, at a special oxygen concentration (higher than 10 pct), Padilla *et al.*<sup>[22]</sup> found that antimony volatilization was inhibited by the formation of a nonvolatile compound,  $SbO_2$ . In the presence of  $As_2O_3$ , the  $Sb_2O_3$  would be transformed into a heteronuclear compound  $As_xSb_yO_6$  (where  $x = 1, 2$ , or 3, and  $x + y = 4$ ) during the roasting process, and it would inhibit the arsenic volatilization and simultaneously promote antimony volatilization at 473 K to 1073 K (200 °C to 800 °C).<sup>[17,23,24]</sup> Tang *et al.*<sup>[18]</sup> and Li *et al.*<sup>[19]</sup> researched the separation of arsenic from high arsenic-antimony dusts under  $N_2-O_2$  mixed atmospheres, the results of which showed that less than 61 mass pct of arsenic and higher than 9 mass pct of antimony volatilized into gas phases. It is difficult to separate arsenic and antimony through traditional pyrometallurgical processing, since  $As_2O_3$  and  $Sb_2O_3$  are both easy to volatilize in inert atmosphere and oxidize in a strong oxidizing atmosphere. A higher separation rate of arsenic and antimony could be obtained using the hydrometallurgical process, but it consumes large amounts of reagents and has high operation costs. First, the antimony is deposited in slag, and arsenic is extracted into solution by acid leaching,<sup>[25,26]</sup> alkali leaching,<sup>[27,28]</sup> chlorination leaching,<sup>[29]</sup> or oxidation leaching.<sup>[30]</sup> Then the antimony is separated from the solution by filtration, and the arsenic is deposited from the leaching solution by lime, ferric salt, or sodium sulfide.

Based on the distinctions of volatility and reducibility of arsenic and antimony compounds, this article proposes an environmentally friendly method of selective oxidation to treat the antimony-bearing dust. The CuO was used as an oxidant participating in the roasting, and the influences of processing parameters on separating

DA-PENG ZHONG, LEI LI, and CHENG TAN are with the State Key Laboratory of Complex Non-ferrous Metal Resources Clean Utilization, Engineering Research Center of Metallurgical Energy Conservation and Emission Reduction of Ministry of Education, Faculty of Metallurgical and Energy Engineering, Kunming University of Science and Technology, Kunming 650093, P.R. China. Contact e-mail: tianxiametal1008@163.com

Manuscript submitted July 20, 2016.

Article published online January 11, 2017.

arsenic were investigated systematically, including roasting temperature, roasting time, additional amount of CuO, and N<sub>2</sub> flow rate.

## II. EXPERIMENTAL

### A. Materials

The antimony-bearing dust used in this study was provided by a plant, located in Yunnan province, China, that treats tin anode slime using a pyrometallurgical

**Table I. Chemical Composition of the Antimony-Bearing Dust (Mass Percent)**

Element	As	Sb	O	C	Se	Pb	F
Content	36.28	28.72	22.35	2.52	2.46	2.06	2.05
Element	Fe	Bi	Na	Sn	Cu	SiO <sub>2</sub>	Others
Content	1.13	0.68	0.40	0.25	0.24	0.05	0.81

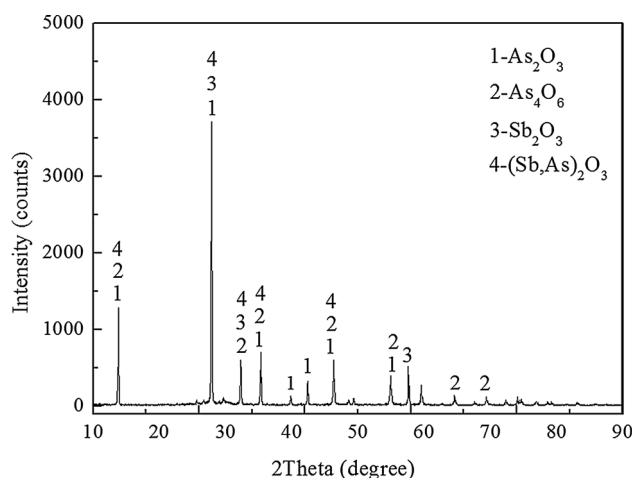


Fig. 1—XRD pattern of the antimony-bearing dust.

process. The chemical composition (mass percent) of the dust is presented in Table I. It shows that the major elements present are arsenic (36.28 mass pct), antimony (28.72 mass pct), and oxygen (22.35 mass pct). “Others” in Table I is mainly composed of “Ca,” “K,” “S,” etc. The main mineral constituents of the dust, established by X-ray diffraction (XRD) and electron probe microanalysis (EPMA), are reported in Figures 1 and 2. Figure 1 shows that the main phases are As<sub>2</sub>O<sub>3</sub>, Sb<sub>2</sub>O<sub>3</sub>, As<sub>4</sub>O<sub>6</sub>, and (Sb,As)<sub>2</sub>O<sub>3</sub>, and Figure 2 shows that the dust mainly contains phases of arsenic and antimony. Specifically, most arsenic-containing phases occur independently in the form of As<sub>2</sub>O<sub>3</sub>, and most antimony is embedded in arsenic-containing complicated phases (altered red sulfur arsenic antimony sodium ore). Meanwhile, some antimony occurs in the form of Sb<sub>2</sub>O<sub>3</sub> at every size fraction. The CuO reagent was used as the oxidant in the roasting process, the CuO content of which was over 99 mass pct.

### B. Roasting Experiments

The experimental apparatus was shown as Figure 3. Five points should be made: (1) the reaction system was set up in a tube furnace (GSL-1500X, Hefei Kejing Materials Technology Co. Ltd., China); (2) the roasting temperature was measured by a Pt-Rh thermocouple and controlled by a KSY Intelligent Temperature Controller (accuracy ±1 °C); (3) pure N<sub>2</sub> was led into the quartz tube during the entire experiment; (4) 5 g of antimony-bearing dust was used in every experiment; and (5) the additional amount of CuO was computed based on its mass ratio to the antimony-bearing dust used, the range of which researched was from 18.18 to 38.36 mass pct.

Three steps were conducted in the roasting tests. First, the antimony-bearing dust and CuO were mixed fully. Second, mixtures of antimony-bearing dusts and CuO were roasted in the tube furnace for 25 to 125 minutes at 623 K to 723 K (350 °C to 450 °C) under N<sub>2</sub> atmosphere when the temperature reached a constant value. The off-gas from the reaction tube was continuously passed

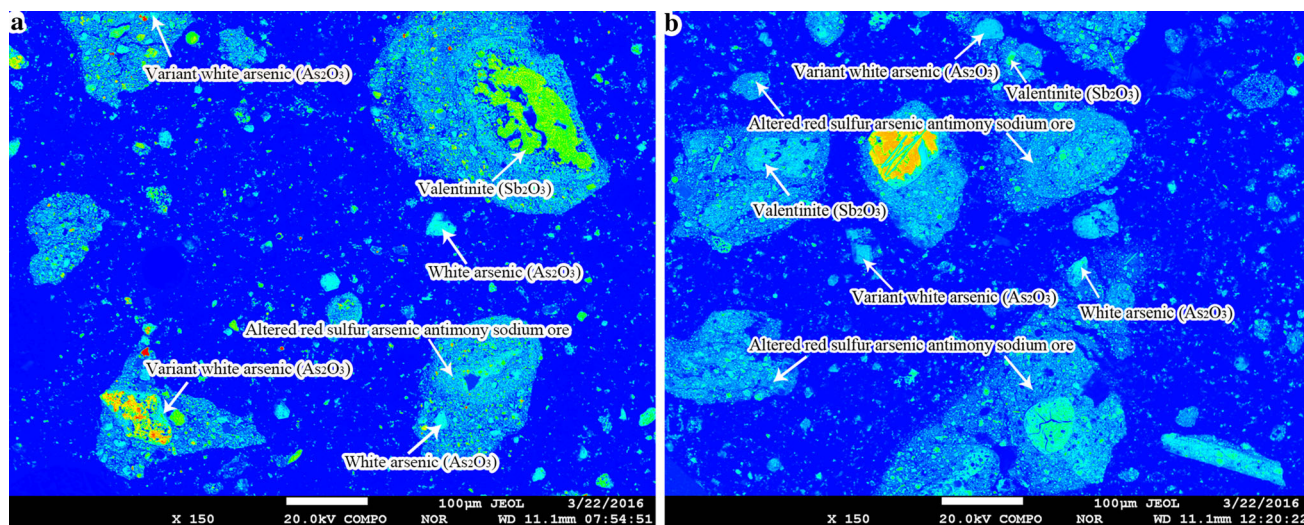


Fig. 2—Mineral phase of distribution of the antimony-bearing dust obtained by EPMA: (a) concentrates particle size of 0.075 mm; (b) concentrates particle size of 0.061 mm.

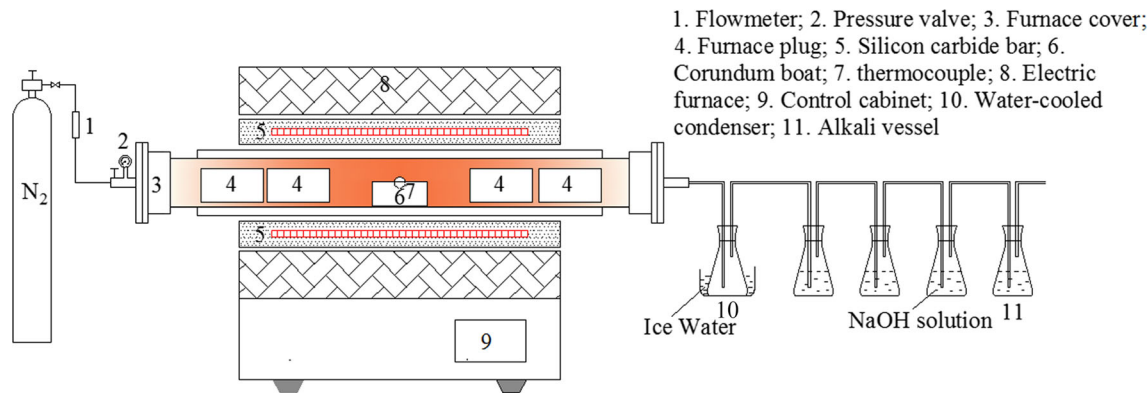


Fig. 3—Experimental apparatus.

through a water-cooled condenser, which collected the volatile matter, and then was directed to solutions of 1 M NaOH to remove harmful components (Figure 3). Finally, after a proper time held, the roasted residue was cooled in the tube furnace to room temperature under  $N_2$  atmosphere and then was pulled out for analysis.

### C. Characterization

The thermogravimetric (TG) analysis and differential scanning calorimetry (DSC) of the samples were performed in a thermal analyzer (NETZSCH, STA 449 F3). The typical measurements were performed at a heating rate of 0.083 K/s under  $N_2$  atmosphere. Chemical composition and mineralogy of the samples were characterized by chemical analysis and EPMA. Especially, an XRF analysis (MINIPAL4, PANalytical, Netherlands) was used to detect the “O” content in the original dust. Phase compositions of all the samples were detected by XRD with Cu  $K_{\alpha}$  radiation (the scanning rate was per 8 deg of 1 minute, and  $2\theta$  was 10 to 90 deg). The thermodynamic data of species were given by FactSage thermochemical software. The mathematical expressions of volatilization rates of arsenic ( $R_A$ ) and antimony ( $R_S$ ) were defined as

$$R_A = \left(1 - \frac{M_T \times W_{A2}}{M_C \times W_{A1}}\right) \times 100 \text{ pct} \quad [1]$$

$$R_S = \left(1 - \frac{M_T \times W_{S2}}{M_C \times W_{S1}}\right) \times 100 \text{ pct} \quad [2]$$

where  $M_C$  stands for the mass of antimony-bearing dust used;  $W_{A1}$  and  $W_{S1}$  for arsenic and antimony contents in the origin antimony-bearing dust, respectively;  $M_T$  for the mass of roasted residues; and  $W_{A2}$  and  $W_{S2}$  for arsenic and antimony contents in the roasted residues, respectively.

## III. THERMOCHEMICAL BEHAVIOR OF THE MIXTURE OF CUO AND ANTIMONY-BEARING DUST

Figure 4 shows TG-DSC curves of CuO, antimony-bearing dusts, and the mixture of them (23.02

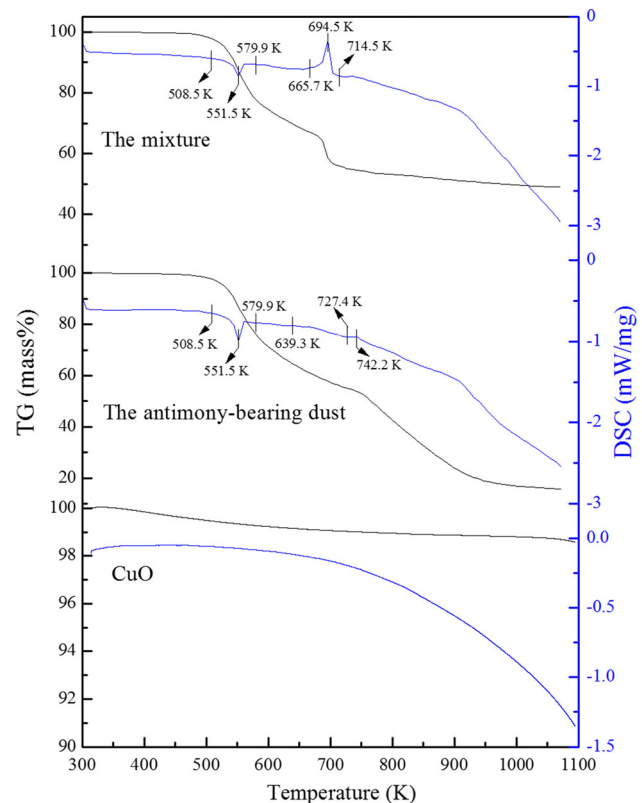


Fig. 4—TG-DSC curves of CuO, antimony-bearing dusts, and the mixture of them (the CuO amount is 23.02 mass pct).

mass pct CuO) under  $N_2$  atmosphere. The CuO is stable in the inspected temperature deduced from its DSC curve, in which there is no obvious endothermic or exothermic peak. Two endothermic peaks located at 508.5 K to 742.2 K (235.5 °C to 469.2 °C) are detected in the DSC measurement for antimony-bearing dust, and each peak corresponds to a mass-loss stage. The first endothermic peak observed at 508.5 K to 579.9 K (235.5 °C to 306.9 °C) is attributed to  $As_2O_3$  phase melting [melting point of  $As_2O_3$  is 548 K (275 °C)<sup>[31]</sup>] and the dust volatilization, and the second peak occurring at 639.3 K to 742.2 K (366.3 °C to 469.2 °C) is attributed to evaporation of the dust. The main evaporations are shown as Eqs. [3] and [4].<sup>[21]</sup> Different

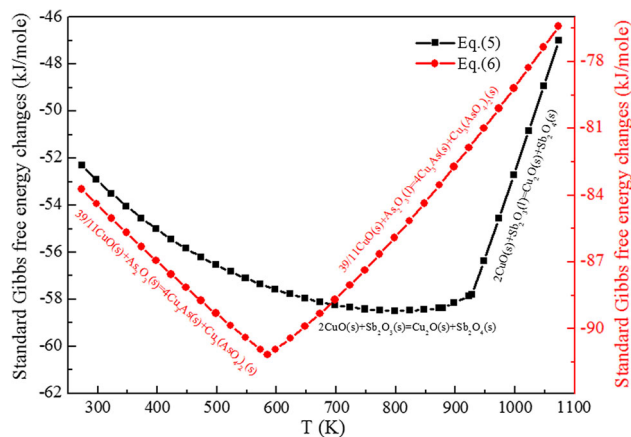


Fig. 5—Standard Gibbs free energy changes of Eqs. [5] and [6] with temperature.

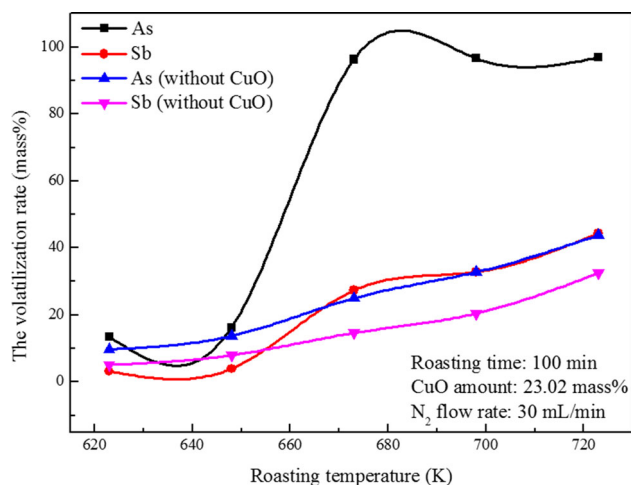


Fig. 6—Effects of roasting temperature on volatilization rates of arsenic and antimony.

from it, the DSC curve for the mixture shows an obvious exothermic peak at 665.7 K to 714.5 K (392.7 °C to 441.5 °C), which may be related to Reactions [5] and [6]. The standard Gibbs free energy changes of Eqs. [5] and [6] with temperature are shown in Figure 5. Meanwhile, the corresponding TG curve shows significant weight loss, which is also ascribed to volatilization of the dust. Mass  $\text{As}_2\text{O}_3$  (s) will be disproportionated into  $\text{Cu}_3\text{As}$  and  $\text{Cu}_3(\text{AsO}_4)_2$  by CuO (Eq. [6]) if Eq. [3] does not largely occur, resulting in the decrease of arsenic volatilization. A suitable temperature and CuO amount are important for separating arsenic from the dust effectively.

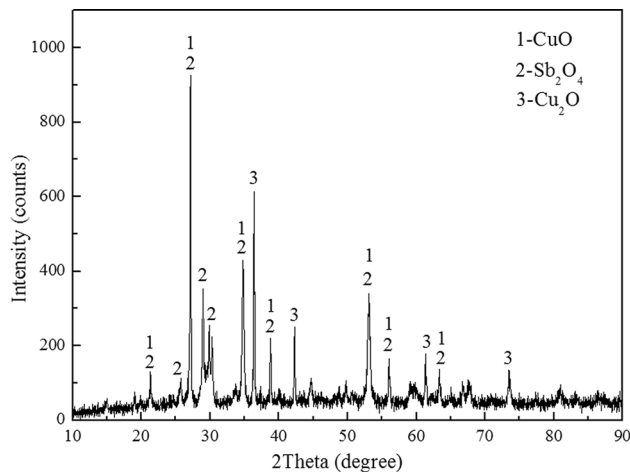
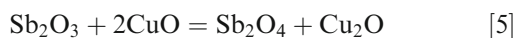
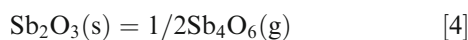
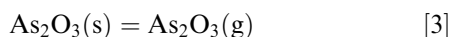
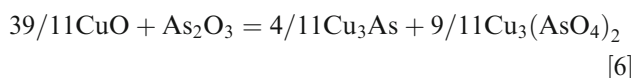


Fig. 7—XRD pattern of the mixture roasted at 673 K (400 °C).



## IV. RESULTS AND DISCUSSION

### A. Effects of Roasting Temperature

Under a  $\text{N}_2$  flow rate of 30 mL/min, roasting time of 125 minutes, and CuO amount of 23.02 mass pct, five roasting temperatures of 623 K, 648 K, 673 K, 698 K, and 723 K (350 °C, 375 °C, 400 °C, 425 °C, and 450 °C) were chosen for studying the effects on the volatilization rates of arsenic and antimony. In addition, a blank test without CuO addition was also carried out with the same condition.

With a CuO amount of 23.02 mass pct, Figure 6 shows that the volatilization rate of arsenic increases from 13.56 to 96.91 mass pct and antimony from 3.18 to 44.31 mass pct, increasing the roasting temperature from 623 K to 723 K (350 °C to 450 °C). Accordingly, the rate for arsenic increases from 9.76 to 43.77 mass pct and antimony from 5.12 to 32.56 mass pct in the blank test. Temperature has an effect mainly on vapor pressures of volatile species, and they increase with temperature. During the roasting process,  $\text{Sb}_2\text{O}_3$  could be oxidized to  $\text{Sb}_2\text{O}_4$  and the  $\text{As}_2\text{O}_3$  disproportionated into  $\text{Cu}_3\text{As}$  and  $\text{Cu}_3(\text{AsO}_4)_2$  through Eqs. [5] and [6]; further, their volatilization rates should be decreased in the presence of CuO. However, they are different from those in Figure 6. The evaporation of  $\text{As}_2\text{O}_3$  appears earlier than in disproportionation on CuO due to its strong volatility, meaning CuO has little negative influence on arsenic evaporation. Meanwhile, structures of some As-Sb complicated phases (altered red sulfur arsenic antimony sodium ore) in the dust (Figure 2) will be destroyed after the “Sb” component within them is oxidized to  $\text{Sb}_2\text{O}_4$  (Figure 7), and this part of arsenic might be transformed to  $\text{As}_2\text{O}_3$  and continue to volatilize, causing the arsenic volatilization rate to be

higher than that in the blank test. In addition, the formation of a heteronuclear compound  $As_xSb_yO_6$  (where  $x = 1, 2, \text{ or } 3$ , and  $x + y = 4$ ) will be hindered after the  $Sb_2O_3$  in the dust is oxidized to  $Sb_2O_4$ ,<sup>[17,23,24]</sup> which also improves  $As_2O_3$  volatilization. Reactions of Eqs. [5] and [6] release heat (Figure 4), which enhances the vapor pressure of the nonoxidative  $Sb_2O_3$  and further leads to the antimony volatilization rate being

higher than that in the blank test at 673 K to 723 K (400 °C to 450 °C). For the purpose of increasing the removal rate of arsenic and reducing antimony loss, the roasting temperature is determined as 673 K (400 °C).

### B. Effects of Roasting Time

The effects of roasting time on volatilization rates of arsenic and antimony were investigated, and the experimental results are presented in Figure 8. It is obvious that the increase of roasting time results in increased volatilization rates for both arsenic and antimony, and the volatilization rate of arsenic is higher than that of antimony because of the difference in their vapor pressures. Precisely, the arsenic volatilization rate increases gradually in the primary 100 minutes, from 5.37 to 95.61 mass pct, and then remains nearly constant. Comparatively, that for antimony always increases, from 4.88 to 27.37 mass pct. For the purpose of increasing separation efficiency of arsenic and antimony, the roasting time is determined as 100 minutes.

### C. Effects of CuO Addition

FactSage 7.0 was used to calculate the phase composition of the roasted product of antimony-bearing dust and CuO. The  $CuO-Sb_2O_3-As_2O_3$  ternary diagram plotted is presented in Figure 9, in which the calculation parameters were set at 1 atm pressure of shielding gas;

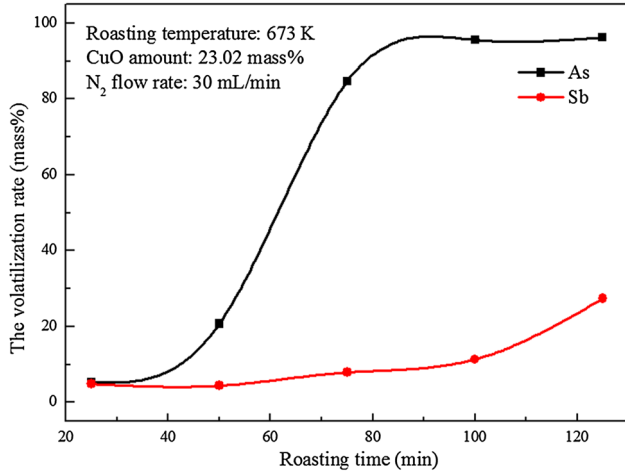


Fig. 8—Effects of roasting time on volatilization rates of arsenic and antimony.

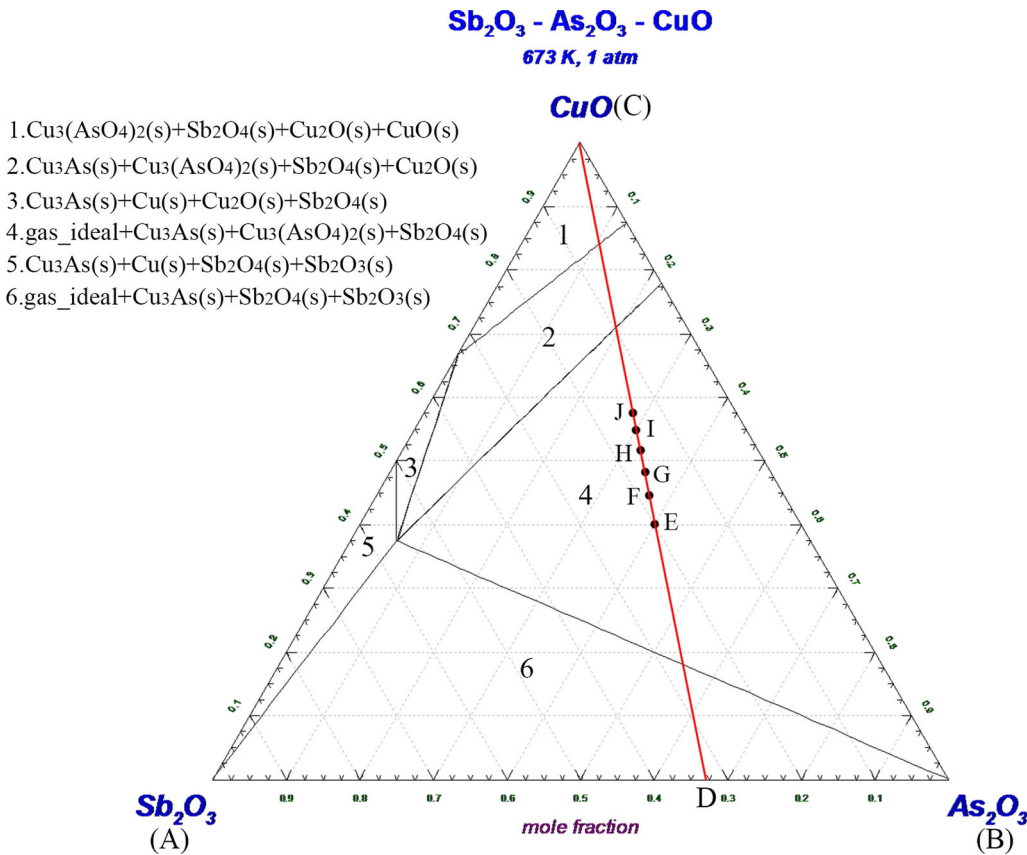
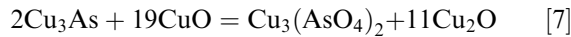


Fig. 9— $CuO-Sb_2O_3-As_2O_3$  ternary diagram at 673 K (400 °C).

the figure shows that the phase changes greatly with CuO. Precisely, amounts of  $\text{Sb}_2\text{O}_4$  and  $\text{Cu}_3(\text{AsO}_4)_2$  increase with the CuO, and  $\text{Cu}_3\text{As}$  decreases from region “6” to “2” and vanishes in region “1,” which may be related to the oxidation of  $\text{Cu}_3\text{As}$  by the excess CuO (Eq. [7]). Besides, the reduction products of CuO change with the CuO amount, which is Cu at a relatively low amount and  $\text{Cu}_2\text{O}$  at a higher amount.



The mole ratio of  $\text{As}_2\text{O}_3$  and  $\text{Sb}_2\text{O}_3$  is fixed at 32.73:67.27 in the antimony-bearing dust, displayed as the line “CD” in Figure 9. It crosses regions “1,” “2,” “4,” and “6.” Increasing the separation efficiency of arsenic and antimony, the  $\text{Sb}_2\text{O}_3$  should be transformed to  $\text{Sb}_2\text{O}_4$ , and simultaneously, the disproportionation of  $\text{As}_2\text{O}_3$  should be restricted. Then region “4” is chosen to be researched. In detail, six CuO additional amounts of 19.18 mass pct (“E” point), 23.02 mass pct (“F” point), 26.86 mass pct (“G” point), 30.70 mass pct (“H” point),

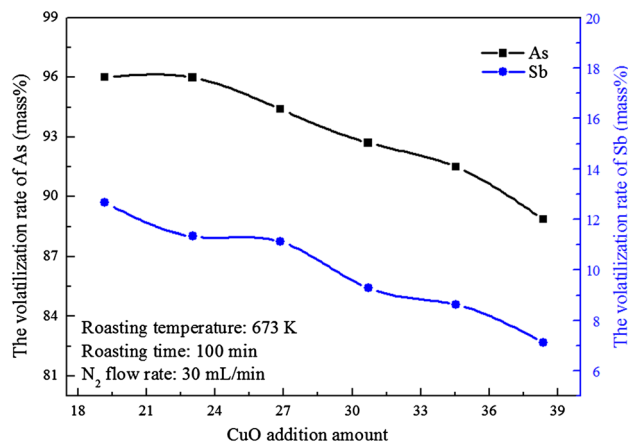


Fig. 10—Effects of CuO amount on volatilization rates of arsenic and antimony.

34.54 mass pct (“I” point), and 38.36 mass pct (“J” point) were selected.

Figure 10 shows that volatilization rates of arsenic and antimony both decrease with the CuO amount. It explains that an excess CuO will cause more formation of  $\text{Cu}_3(\text{AsO}_4)_2$  and  $\text{Cu}_3\text{As}$  and inhibit  $\text{As}_2\text{O}_3$  volatilization (Eq. [6]). However, the  $\text{Cu}_3\text{As}$  is not found in Figure 11, the reason for which may be that  $\text{Cu}_3\text{As}$  was oxidized to CuO and  $\text{As}_2\text{O}_3$  (Eq. [8]) during the sampling preparation for analysis. The antimony volatilization rate decreases smoothly from 12.67 to 7.12 mass pct with a CuO amount of 19.18 to 38.36 mass pct, which indicates that an excess CuO is conducive to decreasing the antimony loss. For the purpose of increasing the separation rate of arsenic and antimony, the CuO addition amount is fixed at 34.54 mass pct.



#### D. Effects of $\text{N}_2$ Flow Rate

With a  $\text{N}_2$  flow rate ranging from 30 to 210 mL/min, Figure 12 shows that the volatilization rate of arsenic remains nearly constant and presents little increase at a  $\text{N}_2$  flow rate higher than 135 mL/min, and that for antimony increases slightly from 8.63 to 10.05 mass pct. The figure explains that the  $\text{N}_2$  flow rate has little effect on the separation of arsenic and antimony, and the external mass transfer does not play a significant role in vaporization of the dust.

For the purpose of increasing separation rates of arsenic and antimony, the preceding results suggest that the selective oxidation roasting of antimony-bearing dust using CuO should be carried out at a roasting temperature of 673 K (400 °C), roasting time of 100 minutes, CuO amount of 34.54 mass pct, and  $\text{N}_2$  flow rate of 30 mL/min. Under these optimum conditions, the volatilization rate of arsenic is about 91.50 pct and that for antimony is only about 8.63 pct. The separation

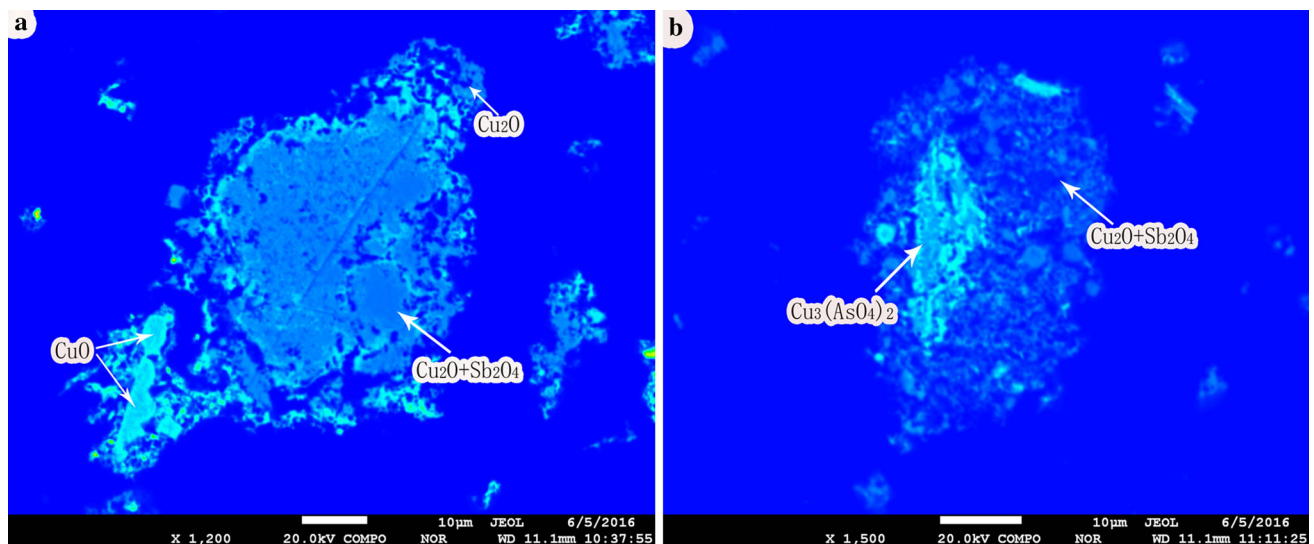


Fig. 11—EPMA of the roasted residue with the CuO amount of 34.54 mass pct [MAG (a): 1200 x; MAG (b): 1500 x].

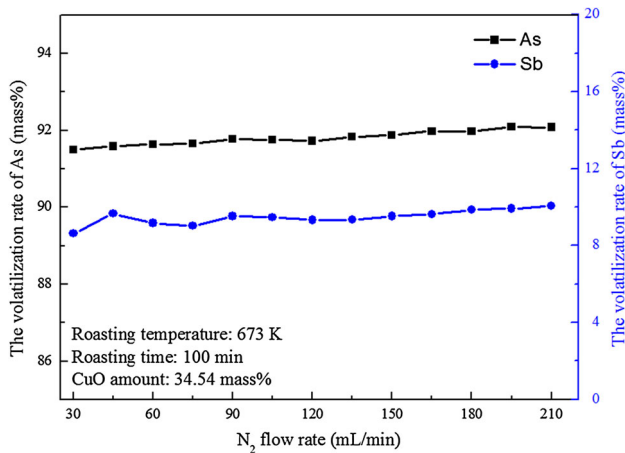


Fig. 12—Effects of N<sub>2</sub> flow rate on volatilization rates of arsenic and antimony.

rate of arsenic and antimony in this study outclasses that in the previous research using pyrometallurgical or hydrometallurgical processes. In addition, the antimony in the roasted products can be reclaimed through reduction roasting and a dust collection process.<sup>[21]</sup>

## V. CONCLUSIONS

The effective removal of arsenic from the antimony-bearing dust through coroasting with CuO is practicable. The factors, including roasting temperature, roasting time, and CuO addition amount, play important roles in the separation of arsenic and antimony, and the N<sub>2</sub> flow rate hardly influences it.

Volatilization rates of arsenic and antimony increase with the roasting temperature and time. The strong volatility of As<sub>2</sub>O<sub>3</sub> results in its evaporation if it happens before being disproportionated into Cu<sub>3</sub>As and Cu<sub>3</sub>(AsO<sub>4</sub>)<sub>2</sub>, and the CuO has a slight negative influence on the arsenic evaporation. On the contrary, structures of some complicated As-Sb phases in the dust will be destroyed after the “Sb” component in them is oxidized to Sb<sub>2</sub>O<sub>4</sub>, and this part of arsenic might be transformed to As<sub>2</sub>O<sub>3</sub> and continue to volatilize; as a result, the As<sub>2</sub>O<sub>3</sub> evaporation is promoted. However, in a certain range, the arsenic volatilization rate decreases with the CuO amount, which is attributed to the greater formation of Cu<sub>3</sub>(AsO<sub>4</sub>)<sub>2</sub> and Cu<sub>3</sub>As. In order to increase the arsenic removal rate and reduce antimony loss, the optimum conditions are established as follows: roasting temperature, 673 K (400 °C); roasting time, 100 minutes; CuO addition amount, 34.54 mass pct; and N<sub>2</sub> flow rate, 30 mL/min. After roasting under these conditions, the antimony in antimony-bearing dusts is transformed into Sb<sub>2</sub>O<sub>4</sub> and its volatilization rate is only 8.63 mass pct; meanwhile, the arsenic removal rate is up to 91.50 mass pct.

## ACKNOWLEDGMENTS

The authors express thanks to the National Science Fund for Distinguished Regional Scholars (Grant No. 51564034) and Scientific and Technological Leading Talent Projects in Yunnan Province (Grant No. 2015HA019) for financial support of this research.

## REFERENCES

1. M. Filella, N. Belzile, and Y.W. Chen: *Earth Sci. Rev.*, 2002, vol. 57, pp. 125–76.
2. X. Wang, J.P. Wang, C.H. Liu, and F.F. Zhang: *China Met. Bull.*, 2014, vol. 23, pp. 6–10 (in Chinese with English abstract).
3. M.C. He, X.Q. Wang, F.C. Wu, and Z.Y. Fu: *Sci. Total Environ.*, 2012, vols. 421–422, pp. 41–45.
4. H. Binz and B. Friedrich: *Chem. Ing. Tech.*, 2015, vol. 87, pp. 1569–79.
5. M. Lundgren, U. Leimalm, G. Hyllander, L.S. Ökvist, and B. Björkman: *ISIJ Int.*, 2010, vol. 50, pp. 1570–80.
6. R.A. Shawabkeh: *Hydrometallurgy*, 2010, vol. 104, pp. 61–65.
7. Y.L. Zhang and E. Kasai: *ISIJ Int.*, 2005, vol. 45, pp. 1813–19.
8. C.S. Chen, Y.J. Shih, and Y.H. Huang: *Waste Manag.*, 2016, vol. 52, pp. 212–20.
9. Z.F. Xu, Q. Li, and H.P. Nie: *Trans. Nonferrous Met. Soc. China*, 2010, vol. 20, pp. s176–81.
10. C. Vandecasteele, V. Dutré, D. Geysen, and G. Wauters: *Waste Manag.*, 2002, vol. 22, pp. 143–46.
11. V. Montenegro, H. Sano, and T. Fujisawa: *Miner. Eng.*, 2013, vol. 49, pp. 184–89.
12. Y. Chen, T. Liao, G.B. Li, B.Z. Chen, and X.C. Shi: *Miner. Eng.*, 2012, vol. 39, pp. 23–28.
13. H.L. Yang, M.C. He, and X.Q. Wing: *Environ. Geochem. Health*, 2015, vol. 37, pp. 21–33.
14. M.P. Taylor, S.A. Mould, L.J. Kristensen, and M. Rouillon: *Environ. Res.*, 2014, vol. 135, pp. 296–303.
15. D. Dupont, S. Arnout, P.T. Jones, and K. Binnemans: *J. Sustain. Metall.*, 2016, vol. 2, pp. 79–103.
16. J. Chen, G. Xie, and D.P. Zhao: *Chin. J. Inorg. Anal. Chem.*, 2014, vol. 4, pp. 11–15 (in Chinese with English abstract).
17. G.A. Brooks, W.J. Rankin, and N.B. Gray: *Metall. Mater. Trans. B*, 1994, vol. 25B, pp. 873–84.
18. H.B. Tang, Q.W. Qin, Y. Guo, X. Zheng, P. Xue, and G.Q. Li: *Conserv. Util. Miner. Res.*, 2014, vol. 3, pp. 35–38 (in Chinese with English abstract).
19. L. Li, R.J. Zhang, B. Liao, and X.F. Xie: *Chin. J. Process Eng.*, 2014, vol. 14, pp. 71–77 (in Chinese with English abstract).
20. HB Yuan, YY Zhu, and JB Zhang: *J. Central South Univ. (Sci. Technol.)*, 2013, vol. 44, pp. 2200–05 (in Chinese with English abstract).
21. A. Aracena, O. Jerez, and C. Antonucci: *Trans. Nonferrous Met. Soc. China*, 2016, vol. 26, pp. 294–300.
22. R.P. Padilla, G. Ramírez, and M.C. Ruiz: *Metall. Mater. Trans. B*, 2010, vol. 40B, pp. 1284–92.
23. J.E. Mauser: *Metall. Mater. Trans. B*, 1982, vol. 13B, pp. 511–13.
24. G.A. Brooks, W.J. Rankin, and N.B. Gray: *Metall. Mater. Trans. B*, 1994, vol. 25B, pp. 865–71.
25. J.S. Wang: *Copper Ind. Eng.*, 2005, vol. 1, pp. 27–28 (in Chinese with English abstract).
26. S. Kashiwakura, H. Ohno, K. Matsubae-Yokoyama, Y. Kumagai, H. Kubo, and T. Nagasaka: *J. Hazardous Mater.*, 2010, vol. 181, pp. 419–25.
27. X.Y. Guo, J. Shi, Y. Yia, Q.H. Tian, and D. Li: *J. Environ. Chem. Eng.*, 2015, vol. 3, pp. 2236–42.
28. I. Mihajlovic, N. Strbac, Z. Zivkovic, R. Kovacevic, and M. Stehernik: *Miner. Eng.*, 2007, vol. 20, pp. 26–33.
29. X.X. Jiang, G.X. He, X.G. Li, and Q. Lu: *Hydrometall. China*, 2010, vol. 29, pp. 199–202 (in Chinese with English abstract).
30. E. Vircikova and M. Havlik: *JOM*, 1999, vol. 51, pp. 20–23.
31. FactSage 7.0: *FactPS—FACT Pure Substances Database*, Thermfact/CRCT and GTT Technologies, 2015.